

Ground-motion prediction equation for South Korea based on recent earthquake records

Ki-Hyun Jeong* and Han-Seon Lee^a

School of Civil, Environmental and Architectural Engineering, Korea University, Seoul 02841, Korea

(Received December 19, 2017, Revised March 21, 2018, Accepted March 22, 2018)

Abstract. A ground-motion prediction equation (GMPE) for the Korean Peninsula, especially for South Korea, is developed based on synthetic ground motions generated using a ground motion model derived from instrumental records from 11 recent earthquakes of $M_L > 4.5$ in Korea, including the Gyeongju earthquake of Sept. 12, 2016 ($M_L 5.8$). PSAs of one standard deviation from the developed GMPE with $M_w 6.5$ at hypocentral distances of 15 km and 25 km are compared to the design spectrum (soil condition, S_B) of the Korean Building Code 2016 (KBC), indicating that: (1) PSAs at short periods around 0.2 sec can be 1.5 times larger than the corresponding KBC PSA, and (2) SD's at periods longer than 2 sec do not exceed 8 cm. Although this comparison of the design spectrum with those of the GMPE developed herein intends to identify the characteristics of the scenario earthquake in a lower-seismicity region such as South Korea, it does not mean that the current design spectrum should be modified accordingly. To develop a design spectrum compatible with the Korean Peninsula, more systematic research using probabilistic seismic hazard analysis is necessary in the future.

Keywords: ground motion prediction equation; ground motion model; lower-seismicity region; Korean Peninsula

1. Introduction

The ground-motion prediction equations (GMPEs, or ground-motion relations) estimating peak ground motions (such as PGA, PGV, and PGD) and pseudo spectral acceleration (PSA) as functions of earthquake magnitude and distance are an important tool for the earthquake hazard analysis in the field of structural engineering. For high seismicity regions such as California in North America, GMPEs are developed using empirical regression analyses with databases containing ground-motion records (Boore and Atkinson 2008, Boore *et al.* 2014) with respect to earthquake magnitudes, distance, fault types, site conditions, and so on.

For low-to-moderate seismicity regions such as eastern North America (ENA), earthquake records are insufficient within the magnitude and distance range of engineering interest to develop GMPEs by empirical regression analysis (Atkinson 2008, Zuccolo *et al.* 2017). Fig. 1 shows instrumental records with respect to the local magnitude and epicentral distance in Korea. The magnitude and distance range of engineering interest in seismic hazard analysis is $M \geq 6$, and $R \leq 50$ km (Atkinson 2008), but there is lack of records in this range as shown in Fig. 1, which is common in lower seismicity regions, so large uncertainty exists for the design conditions of the empirical attenuation relations (Darragh *et al.* 2015). Due to this lack of critical data, the GMPEs for low-to-moderate seismicity regions were

developed using simulation techniques. (Boore 2015, Pezeshk *et al.* 2011) or hybrid empirical method, which uses host-to-target adjustment factors to adjust empirical attenuation relations in the host region to use in the target region. (Campbell 2003, 2014, Pezeshk *et al.* 2015). However, only recorded earthquake ground motions in the Korean Peninsula are used in this study.

A procedure of the simulation technique of time series is given by Boore (2003) as follows: (1) Gaussian random (or white) noise is generated for given duration; (2) the noise is then band-limited and windowed; (3) this noise is transformed into frequency domain; (4) the Fourier spectrum is normalized; (5) the normalized spectrum is multiplied by the target ground motion spectrum; (6) the resulting spectrum is transformed into the time domain. To complete this procedure, the target ground motion spectrum is determined. Usually the target spectrum is defined by a ground motion model (GMM). This simulation technique with GMM to generate synthetic accelerograms for lower-to-moderate seismicity regions is introduced in detail by Lam *et al.* (2000), Boore (2003).

GMMs are established by investigating the characteristics of the earthquake source, the path effect on the wave propagation including duration, and the site effects. GMMs have the shape of a Fourier spectrum as a function of the earthquake magnitude and distance, while GMPEs have the shape of a response spectrum. For engineering use, the Fourier spectral data of the ground motions should be converted into response spectra and time domain data such as PSA, PGA, and PGV. For low-to-moderate seismicity regions such as ENA, parameters of GMM are derived from several well recorded earthquakes (Boore *et al.* 2010, Boore 2015).

Two example studies for GMPE in Korea were

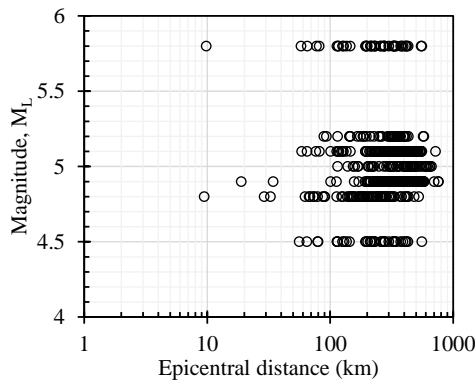
*Corresponding author, Ph.D. Student

E-mail: ghasposcale@korea.ac.kr

^aProfessor

Table 1 List of Earthquakes with $M_L > 4.5$ in the Korean Peninsula

No.	YYYY-MM-DD HH:MM	M_L	M_W	Latitude (°)	Longitude (°)
1	2016-09-19 20:33	4.5	4.6*	35.74	129.18
2	2016-09-12 20:32	5.8	5.4*	35.76	129.19
3	2016-09-12 19:44	5.1	4.9*	35.77	129.19
4	2016-0 -05 20:33	5	4.97	35.51	129.99
5	2014-04-01 04:48	5.1	5.1	36.95	124.5
6	2013-05-18 07:02	4.9	4.85	37.68	124.63
7	2013-04-21 08:21	4.9	4.85	35.16	124.56
8	2007-01-20 20:56	4.8	4.72*	37.68	128.59
9	2004-05-29 19:14	5.2	5.2	36.8	130.2
10	2003-03-30 20:10	5	4.97	37.8	123.7
11	2003-03-23 05:38	4.9	4.85	35	124.6

Fig. 1 Distribution of instrumental records of event $M_L \geq 4.5$ with respect to magnitude and epicentral distance in Korea

conducted by Jo and Baag (2003), and by Emolo *et al.* (2015). The study by Jo and Baag (2003) used records from 16 earthquakes in south-eastern Korea, with the local magnitude ranging from 2.1 to 3.9. Whereas a simulation technique was used to develop the GMPE by Jo and Baag (2003), the GMPE by Emolo *et al.* (2015) is developed using empirical regression analyses of a database of 222 earthquake records with the local magnitudes ranging from 2.0 to 5.1. Therefore, the GMPE by Emolo, *et al.* (2015) can not be extended to estimate ground motions with local magnitudes larger than 5.1.

An earthquake with the local magnitude, M_L 5.8 (M_W 5.4) occurred on Sept. 12, 2016 in Gyeongju City in southern Korea. This is the largest event since 1978 when the Korean seismic instrumental recording began, and it provides a unique opportunity to examine the properties of moderate earthquakes in the Korean Peninsula. In this study, the characteristics of instrumented earthquakes in Korea including the Gyeongju earthquake are accounted for to develop the GMM in the Korean peninsula.

The purpose of this study is (1) to propose the appropriate values of GMM parameters for the Korean Peninsula using recorded data of $M_W \geq 4.5$ earthquakes, and to simulate strong ground motions with $M_W \geq 6.0$ using this GMM. A tool of stochastic method of simulation (SMSIM, Boore 2005) is used to generate ground motions with this GMM and their parameters, and (2) to develop GMPE by

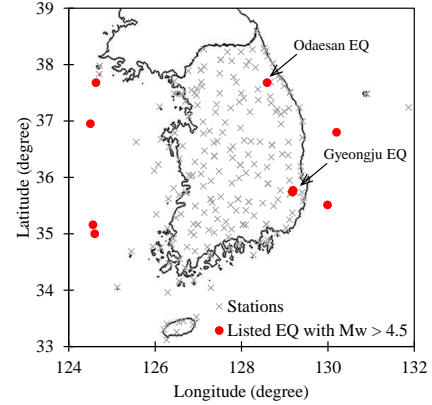


Fig. 2 Locations of stations in Korea and epicenters of listed earthquakes

using the simulated ground motions with the moment magnitude ranging from 4.5 to 6.5 within a distance of 800 km. Finally (3) the 5% damped response spectral accelerations predicted by this GMPE are compared to the KBC (Korean Building Code 2016) design spectrum to see the major difference between the PSAs based on the GMPE and the current design spectrum.

The GMPE allows estimation of the median ground motion and its uncertainty. The uncertainty, generally referred to as the standard deviation (σ) of GMPE, exerts a strong influence on the results of probabilistic seismic hazard analysis (PSHA) (Atik *et al.* 2010).

2. A GMM for the Korean Peninsula

2.1 Instrumental earthquake data in Korea

The Korean seismic instrumental recording began in 1978. However, the earthquake accelerograms that are used were recorded after 2001, because those accelerograms recorded before 2001 have not been uploaded to earthquake database in Korea. Accelerograms from 11 earthquakes, listed in Table 1, with $M_L \geq 4.5$ from a database of the National Earthquake Comprehensive Information System (NECIS), Korean Meteorological Administration (KMA), and Korea Institute of Geoscience and Mineral Resources (KIGAM) are used to determine the GMM parameters for each of the earthquakes. Earthquakes with a magnitude less than 4.5 are not accounted for in developing the GMM, because they do not usually cause damage to building structures (Frankel 1995). NECIS, KMA and KIGAM use the local magnitude, M_L , to describe the magnitudes of earthquake (Table 1). Some moment magnitudes, M_W , of the earthquakes listed in Table 1 are extracted from USGS (denoted with *), and the others of those are calculated using Eq. (1), as suggested by Choi, *et al.* (2004).

$$M_W = 1.92 - 0.04M_{KMA} + 0.13M_{KMA}^2 \quad (1.7 \leq M_{KMA} \leq 5) \quad (1)$$

Fig. 2 shows the locations of the stations in South Korea and epicenters of the listed earthquakes. Only four events are inland earthquakes, including the Odaesan earthquake (No. 8) and the Gyeongju earthquake events (No. 1, 2, and

3 in Table 1, which are after-, main, and fore-shock, respectively). The listed earthquake records range between $4.5 \leq M_L \leq 5.8$, with an epicentral distance of 9.4 km to 757 km (Fig. 1). 79 of 156 recording stations are obtained by the borehole, which is installed stations to reduce and avoid the effect of noises from traffic, changes in air pressure and temperature, tide, and so on. And this borehole measurements are assumed herein to be on bedrock under the geological environment in the Korean Peninsula (NIMR 2014). In the other stations, with the exception of a few stations, instrumentations are installed on bedrock (KMA). For this reason, all the earthquake records in Korea are assumed to be observed on generic rock ($V_{S,30}=760$ m/s~1,500 m/s).

2.2 Description of the GMM

In the point-source model, the Fourier amplitude spectrum (FAS) of the horizontal ground motion due to the shear-wave propagation in an elastic half-space can be modelled as Eq. (2) (Boore 2003, Lam *et al.* 2000, Yenier and Atkinson 2015)

$$A(M_0, f, R) = E(M_0, f)P(R, f)G(f)I(f) \quad (2)$$

where M_0 is the seismic moment (dyne-cm), R is the source-to-site distance (km), f is the frequency (Hz), $E(M_0, f)$ is the source spectrum, $P(R, f)$ is the path attenuation factor, and $G(f)$ is the upper-crust factor. The type of ground motion is controlled by $I(f)$, defined as $(2\pi fi)^n$, where $i=\sqrt{-1}$ and $n=0, 1, \text{ or } 2$ for displacement, velocity, or acceleration, respectively. Since the moment magnitude, M_w , is usually used rather than the seismic moment, M_0 , as a more familiar measure of the earthquake size, M_w is converted to M_0 using Eq. (3) (Hanks and Kanamori 1979)

$$M_w = \frac{2}{3} \log M_0 - 10.7 \quad (3)$$

2.2.1 The source model

Brune (1970) proposed a simple model, $S(f)$, for the earthquake source, and it can generate the Fourier amplitude spectrum for the displacement of seismic shear waves as given in Eq. (4).

$$S(f) = \frac{1}{1 + (f/f_c)^2} \quad (4)$$

The corresponding Fourier amplitude spectrum for specified magnitude is given in Eq. (5).

$$E(M_0, f) = CM_0 S(f) = \frac{CM_0}{1 + (f/f_c)^2} \quad (5)$$

where the corner frequency f_c (Hz) can be related to the stress drop or parameter, $\Delta\sigma$ (bar) by the following Eq. (6)

$$f_c = 4.9 \times 10^6 \beta (\Delta\sigma / M_0)^{1/3} \quad (6)$$

where f_c is in Hz, β (the shear-wave velocity in near the source) in km/s, $\Delta\sigma$ in bars, and M_0 in dyne-cm. The mid-crust scaling factor, C , in Eq. (5), is given in Eq. (7)

$$C = \frac{R_p V F}{4\pi\rho\beta^3 R_0} \quad (7)$$

where R_p is the wave radiation pattern ($=0.55$), V is the partition of the total shear-wave energy into horizontal components ($=1/\sqrt{2}$), F is the effect of the free surface (taken as 2 in this study), ρ is the density in the vicinity of the source, and R_0 is a reference distance, usually set equal to 1 km. ρ and β are assumed to be 2.7 gm/cc and 3.5 km/sec for the Korean Peninsula, respectively, following the values adopted in Jo and Baag (2001, 2003), Ha *et al.* (2016).

2.2.2 The path effect

The path effect is represented by simple functions that account for geometrical spreading, anelastic attenuation, and the general increase of duration with distance due to wave propagation and scattering (Boore 2003). The path effect $P(R, f)$ is given by multiplying the geometrical spreading R^n and $Q(f)=Q_0 f^n$ functions.

$$P(R, f) = R^n \exp\left(\frac{-\pi f R}{Q_0 f^n \beta}\right) \quad (8)$$

Boore, *et al.* (2010) note that the $R^{-1.3}$ rate proposed by Atkinson (2004a) is based on an empirical regression of the FAS from a large Eastern North America (ENA) database of small-to-moderate events, which provide compelling evidence that the geometrical spreading rate within 70 km is faster than R^{-1} .

The anelastic attenuation factor includes all losses that have not been accounted for by the geometrical spreading factor. The Q factor depends on the wave-transmission quality of rock in the region and hence is not unique, and must be determined via seismological monitoring.

The distance-dependence accounts for the decrease in the peak motions with an increasing duration and other things being equal. Although the FAS of the ground motion Eq. (2) is not dependent on the duration, the duration is definitely a function of the path as well as the source. The effective earthquake durations, T_{gm} , can be predicted using the relationship given in Eq. (9).

$$T_{gm} = T_0 + bR \quad (9)$$

where T_0 is the source duration and bR represents a distance-dependent term that accounts for dispersion. The source duration was assumed to be $T_0=1/(2f_c)$. The adopted duration model, which is dependent on the distance, is proposed by Atkinson and Boore (1995) as trilinear, using transition distances of 70 and 130 km for consistency with the attenuation model; the slope b is 0.16 for $10 \leq R \leq 70$ km, -0.03 for $70 < R \leq 130$ km, and 0.04 for $130 \text{ km} < R$. The duration function affects the shape and amplitude of the time-histories and the response spectra of the synthetic ground motions.

2.2.3 The site effect in generic rock

The site effects involve the amplification and attenuation of seismic wave in the upper crust. The modification of seismic waves by the local site conditions can be separated the attenuation and amplification as given

in Eq. (10).

$$G(f) = D(f)A(f) \quad (10)$$

where $D(f)$ is a attenuation factor, and $A(f)$ an amplification factor of the site. The site effects depend on the type of earth structures.

The amplification factor $A(f)$ has been usually defined using the following relationship as given in Eq. (11) (Boore and Joyner 1997).

$$A(f) = \sqrt{\frac{\rho_A \beta_A}{\rho_B \beta_B}} \quad (11)$$

where ρ_A , ρ_B , and β_A , β_B are the densities and the shear wave velocities respectively at the earthquake source (_A) and the site (_B). Eq. (11) is based on the quarter-wavelength approximation introduced by Joyner *et al.* (1981). ρ_A and β_A are constant values as given in Eq. (7). ρ_B and β_B are a function of the frequency and depth, which is related with the velocity profiles (Boore and Joyner 1997). However, the adopted frequency dependent amplification factors $A(f)$ for S_B in Korea proposed by Kim and Yoon (2006) are derived by comparing PSAs, simulated by using the software, SHAKE, on very hard rock and generic rock with V_S profiles at specific sites.

In the upper crust, wave amplitudes decay rapidly, and rocks within 4 km of the earth surface have been found to possess significantly poorer wave transmission qualities compared to rocks at greater depths in California (Lam *et al.* 2000). This attenuation appears to be independent of distances. The attenuation (or diminution) function, $D(f)$ in Eq. (10) accounts for the high-frequency path-independent decay of the ground motions, as given in Eq. (12). (Anderson and Hough 1984)

$$D(f) = e^{-\pi f \kappa_0} \quad (12)$$

The frequency dependent attenuation factor, κ (like anelastic attenuation with $Q(f)$) includes the losses, that have not been accounted for by geometrical spreading. It contains a distance dependent κ_R and independent values κ_0 . κ_R is related to the Q function, but is not used in this study because $Q(f)$ is derived by another approach described in Section 2.3.3. κ_0 represents the loss due to a site effect (Hanks 1982), or by a combination of source and site effect (Boore 2003).

2.3 Determination of GMM parameters from earthquake records in Korea

2.3.1 Evaluation of the site effects in generic rock

The high-frequency decay factor, κ is derived from the FAS of the earthquake records. Hanks (1982) suggests that, in general, the acceleration spectrum decays rapidly above f_{max} , which is a corner frequency between the acceleration and velocity-constant region. Fig. 3 shows a predominantly exponential decrease in the spectral amplitude. Based on Fig. 3, f_{max} is selected for this record to be about 10 Hz. Frequencies higher than 25 Hz are considered as potentially unreliable because some records shows extraordinarily large amplitudes at frequencies above 25 Hz. κ is defined as the

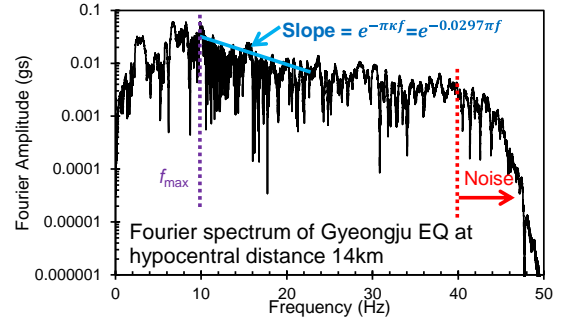


Fig. 3 Fourier amplitude spectrum of the EW component of Gyeongju earthquake recorded at the USN station

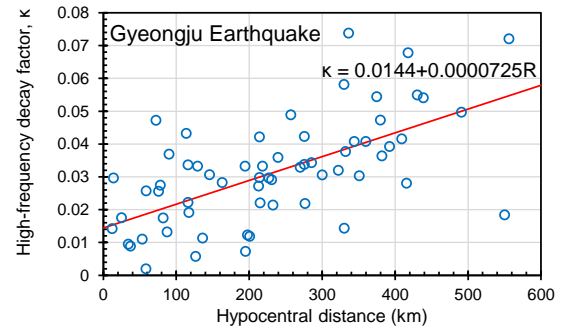


Fig. 4 Values of κ for the frequency band 10 to 25 Hz derived from the Gyeongju earthquake accelerograms

Table 2 κ_0 's of the listed earthquakes (unit: 10^{-4} sec)

No.	1	2	3	4	5	6	7	8	9	10	11
κ_0	179	114	156	145	110	145	145	139	145	145	145

Table 3 Site amplification factors for the site classification B ($V_{S,30}=750$ m/s~1,500 m/s)

f (Hz)	1	2	5	7	10	20	50
Amp.	1	1.05	1.1	1.2	1.6	1.5	1.3

spectral decay slope between the frequencies of 10 Hz and 25 Hz in this study. κ_0 of 0.0144 and κ_R of 0.0000725 are derived by the regression in Fig. 4. The hypocentral distance, R (Fig. 4) is calculated by the assumption of the focal depth of 10 km. As mentioned earlier, κ_R is neglected. κ_0 values for 11 earthquakes are listed in Table 2. However, the κ_0 values of the offshore earthquakes are too much larger than those of inland earthquakes to use for the GMM. Thus, the mean value of κ_0 for inland earthquakes is used instead of actual calculated values (denoted as *Italic*) in Table 2.

The site amplification factors in Table 3 proposed by Kim and Yoon (2006) are adopted in this study. Kim and Yoon (2006) performed site response analysis using the SHAKE program to estimate the site-specific earthquake ground motions at 162 site around the Korean Peninsula, and then calculated the site coefficients for the seismic design using the ratio of the response spectra of the soil and rock.

2.3.2 Determination of geometrical spreading

In the study by the EPRI (1993), the geometrical

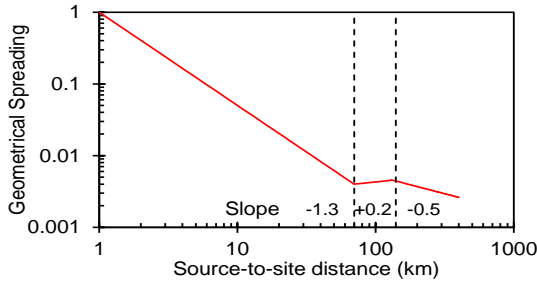


Fig. 5 Geometrical spreading proposed by Atkinson (2004a)

spreading rates are modelled by investigating the earth structures for North America. This theoretical model was not derived from the investigation of the amplitude decay depending on the distance. The path effect is divided into a geometrical spreading and an anelastic attenuation model that includes all amplitude decays that have not been accounted for in the geometrical spreading.

A geometrical spreading rate of R^{-1} has been commonly used within distance of 100 km for the Korean Peninsula (Jo and Baag 2003). However, the $R^{-1.3}$ model is used for the ENA region, a moderate-seismicity and stable continental region similar to the Korean Peninsula, because the attenuation of the earthquake accelerograms of the ENA shows a faster decay than R^{-1} (Boore *et al.* 2010).

A geometrical spreading is modelled based on an investigation of the distributions of the PGA and PSAs of the Odaesan (Jan.20.2007, M_w 4.7) and the Gyeongju (Sept.12.2016, M_w 5.4) earthquakes. Fig. 6 shows the distributions of the PGAs and PSAs ($T=0.1$ s, 0.2 s, 1 s, 5 s, and 10 s) of the Odaesan earthquake records. PSAs with periods of 0.1 s and 0.2 s, and the PGAs show faster decay than R^{-1} . However, the PSAs with a period of 1s or longer show a decay between R^{-1} and $R^{-1.3}$ within a distance of 100

Table 4 Geometrical spreading models

M1
R^{-1} for $R < 100$ km
$R^{-0.5}$ for $R > 100$ km
M2
R^{-1} for $R < 70$ km
R^0 for $70 \text{ km} < R < 130 \text{ km}$
$R^{-0.5}$ for $130 \text{ km} < R$
M3 (Atkinson, 2004a)
$R^{-1.3}$ for $R < 70$ km
$R^{-0.2}$ for $70 \text{ km} < R < 130 \text{ km}$
$R^{-0.5}$ for $130 \text{ km} < R$

km.

For the Gyeongju earthquake records, decays of the PGA and PSA with periods of 0.1 s and 0.2 s also appear to be faster than R^{-1} as shown in Fig. 7. The distribution of the PSA with a period of 0.2 s shows “offset of decay” in the range of distance of 70 km to 200 km. This feature appears more clearly in the distribution of the PSA with periods of 1 s, 5 s and 10 s. Beyond 200 km, the decays become faster, but less than the initial decay.

According to observation of the attenuation characteristic of the Odaesan and Gyeongju earthquake records in Figs. 6 and 7, a geometrical spreading model, $R^{-1.3}$, rather than a simple decay of R^{-1} in a whole range of distance is more appealing. Therefore, the $R^{-1.3}$ model, depicted in Fig. 5, is adopted for the near-source distance in this study.

To verify the geometrical spreading models, 200 synthetic seismograms are generated for each distance by using SMSIM (Boore 2005) with three geometrical spreading models, as presented in Table 4. The offset of decay in the distance ranging from 70 km to 130 km is

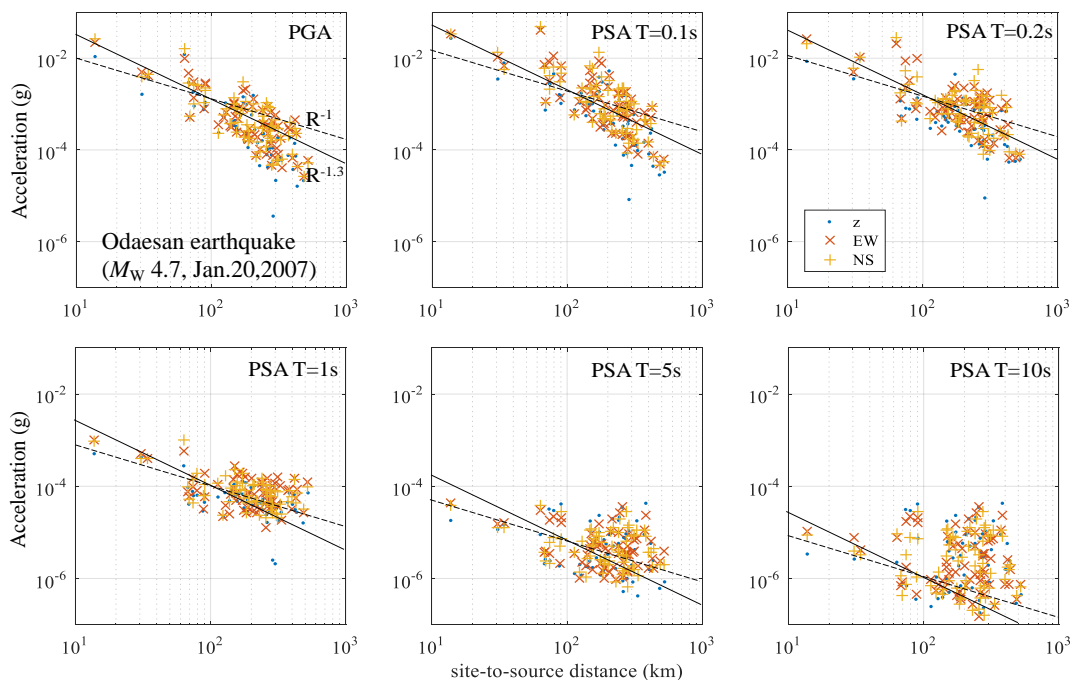


Fig. 6 PGA and PSA distributions of Odaesan earthquake. Solid lines: $R^{-1.3}$ decay, dotted lines: R^{-1} decay

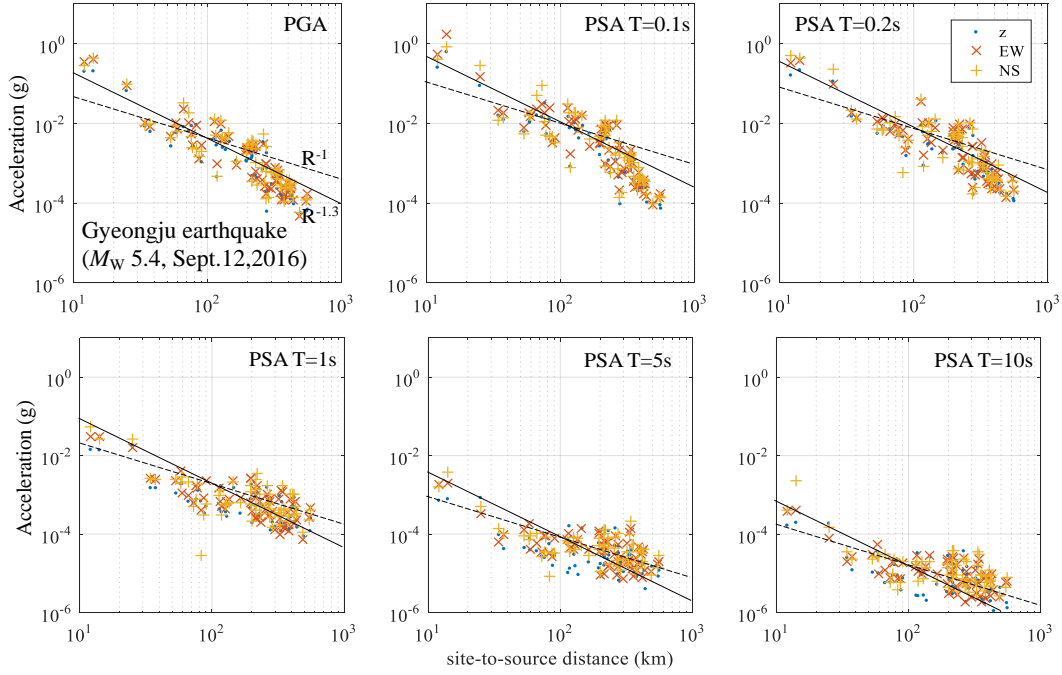


Fig. 7 PGA and PSA distributions of Gyeongju earthquake. Solid lines: $R^{-1.3}$ decay, dotted lines: R^{-1} decay

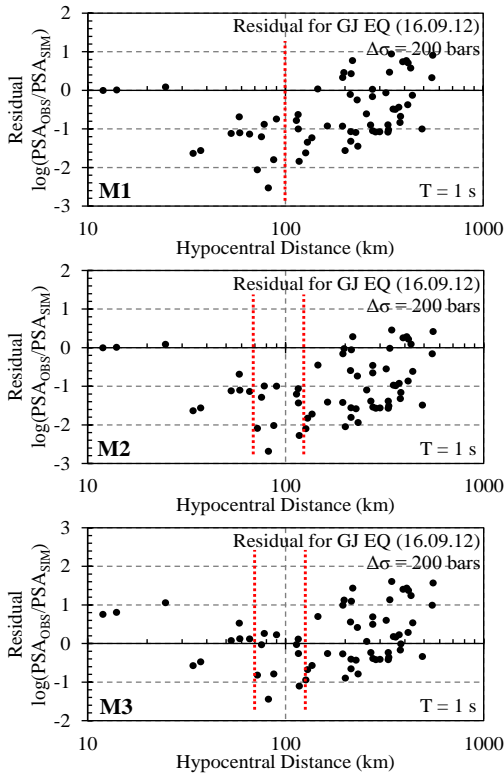


Fig. 8 Residual distribution of Gyeongju (GJ) earthquake

accounted for in $M2$ and $M3$. The residuals, defined as $\log_{10}(PSA_{OBS}/PSA_{SIM})$ at period of 1 s, where PSA_{SIM} is the mean value, are shown in Fig. 8. While the distribution of residual by $M1$ has a downward deviation within 100 km, those by $M2$ also have a wide downward deviation within 130 km, and those by $M3$ suggested by Atkinson (2004a) and shown in Fig. 5 are more evenly distributed than those by $M1$ and $M2$ about the horizontal line.

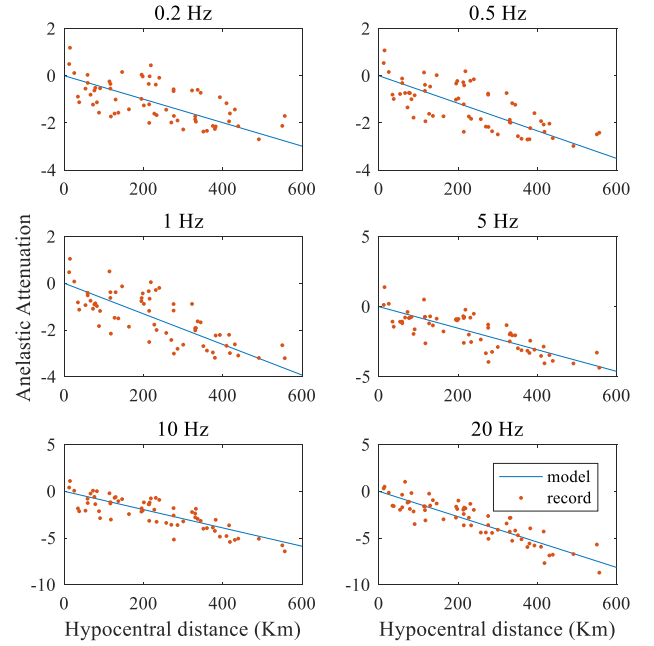


Fig. 9 Anelastic attenuation factor, $Q(f)=238f^{0.602}$ for the Gyeongju earthquake

2.3.3 Evaluation of the anelastic attenuation

The $Q(f)$ function is modeled by using the GMM and its associated values of parameters predetermined for geometrical spreading, site effects, and tentative stress parameter=200 bars, which is a reasonable value for the intraplate regions (Atkinson and Boor 1995). The inversion using this GMM (Eq. (2)) is given in Eq. (13).

$$\exp\left(\frac{-\pi fR}{Q_0 f^\eta \beta}\right) = A_{OBS} / \left[\frac{CM_0 (2\pi f)^2}{1+(f/f_c)^2} R^n e^{-\pi f \kappa_0} \sqrt{\frac{\rho_A \beta_A}{\rho_B \beta_B}} \right] \quad (13)$$

Table 5 $Q(f)$'s of the listed earthquakes (f unit: Hz)

No.	1	2	3	4	5	6	7	8	9	10	11
Q_0	177	238	229	221	368	606	318	436	552	581	582
η	0.71	0.60	0.65	0.66	0.58	0.45	0.60	0.47	0.46	0.46	0.44

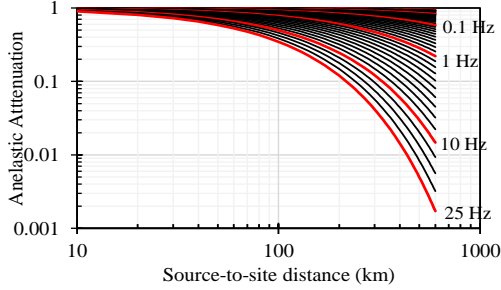
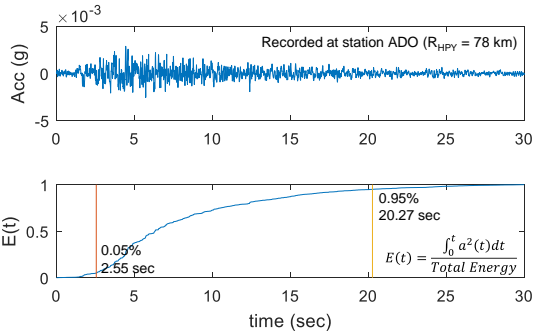

 Fig. 10 Anelastic attenuation factor, $Q(f)$


Fig. 11 Calculation of the rms duration of the acceleration for a record at station ADO (EW component of the Gyeongju earthquake)

Fig. 9 shows results of the Gyeongju earthquake data at frequencies of 0.2, 0.5, 1, 5, 10, and 20 Hz. An anelastic attenuation model by $Q(f)$ of $238f^{0.602}$ is indicated by blue lines in Fig. 9.

$Q(f)$'s for each of the 11 earthquakes are listed in Table 5, and the mean value of $Q(f)$ is shown as a function of frequency (Fig. 10), and given in Eq. (14)

$$Q(f) = Q_0 f^\eta = 357 f^{0.554} \quad (14)$$

Fig. 10 shows a fast decay with increasing distance at a frequency of 25 Hz, and slow decay at lower frequencies.

2.3.4 Evaluation of duration model

An rms duration model given by Atkinson and Boore (1995) is adopted. The duration of the window function, t_η , used in the stochastic simulations of time series in SMSIM (Boore 2005) is given in Eq. (15).

$$t_\eta = f_{T_{gm}} \times T_{gm} \quad (15)$$

where T_{gm} is the ground motion duration model given in Eq. (9), and $f_{T_{gm}}$, defined as a factor to convert the box window duration to the exponential, given as 2.0 by Boore (2003). For simulation in this study, the exponential window function is used. Fig. 11 shows an example of simulation with the rms duration by using the EW component of the Gyeongju accelerograms recorded at the ADO station

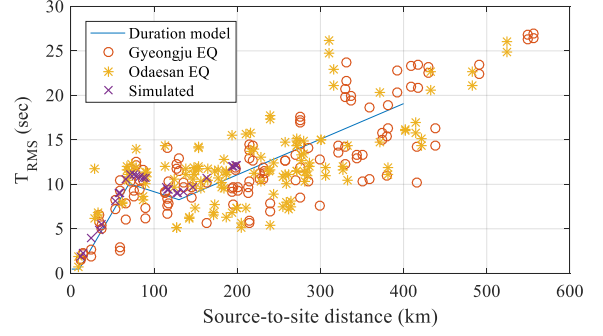
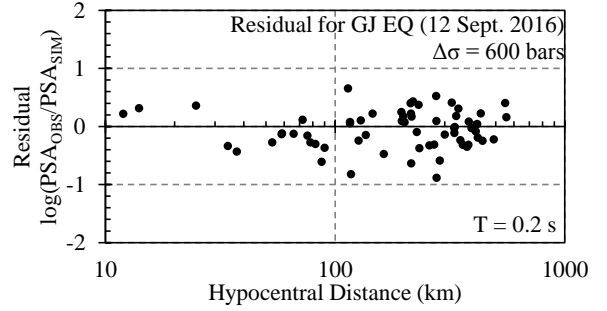

 Fig. 12 Comparison of T_{gm} model and the rms durations of records from Gyeongju and Odaesan earthquakes


Fig. 13 Example of residual distribution of Gyeongju earthquake with stress parameter of 600 bars

(source-to-site distance=78 km). Fig. 12 shows a comparison of duration model T_{gm} , with rms durations of the Gyeongju and Odaesan earthquake records, together with those of simulated accelerograms for reference.

2.3.5 Determination of stress parameter

A stress parameter is needed to model the source effect in Eqs. (5) and (6), and its value is determined to best simulate the near-source ground motion of the listed earthquakes in Table 1 within a distance of 200 km, because (1) at short periods and for most of the attenuation models, the value of stress parameter that leads to the best match of the data for distances within about 200 km leads to an overestimation of the data at greater distances (Pezdech *et al.* 2015), and (2) the damages from the Gyeongju earthquake were found to be concentrated in a small area near the epicenter.

Assuming all the values of the parameters other than the stress parameter are to be fixed, the stress parameter is determined by finding the value of the stress parameter that leads to the least residuals. The first trial value of the stress parameter was 100 bars. If the resulting residual is too large or small, a stress parameter increased or decreased by 10 bars interval has been tried.

PSA_{SIMs} is the mean value of PSA by 200 simulations for each of the earthquake records corresponding to the magnitude and distance of the stations. PSA_{OBSs} are PSAs of the earthquake records. The residual is defined by $\log(PSA_{OBSs}/PSA_{SIMs})$. When the mean value of residuals at a period of 0.2 sec is near the minimum, that value of the stress parameter is selected for each of the earthquake records.

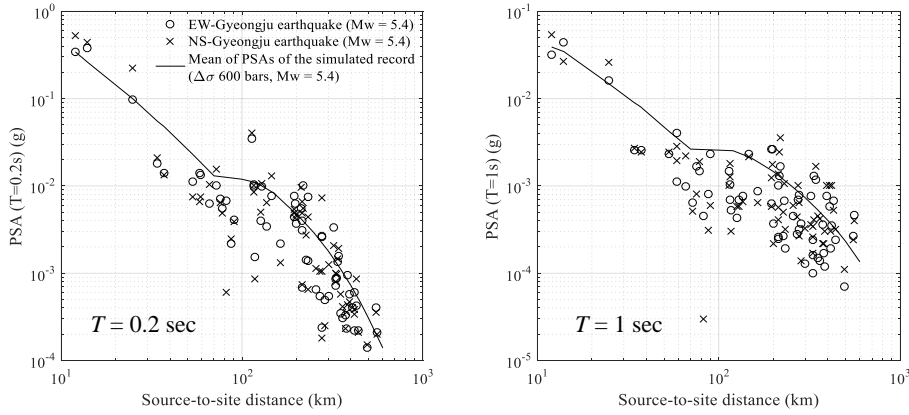


Fig. 14 PSAs of Gyeongju earthquake records and the GMM with stress parameter of 600 bars at periods of 0.2 sec and 1 sec

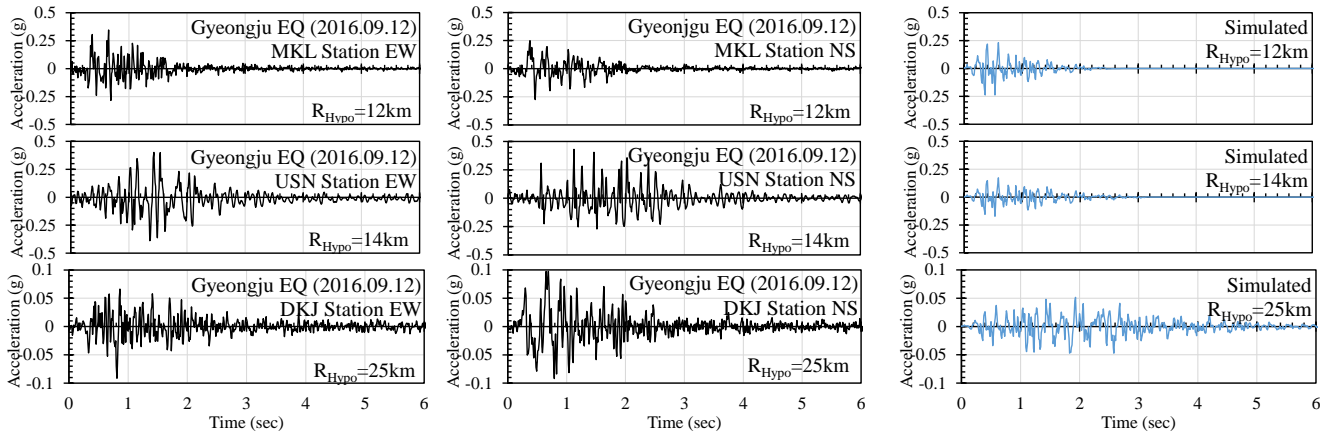


Fig. 15 Time domain accelerograms of GMM and Gyeongju Earthquake records

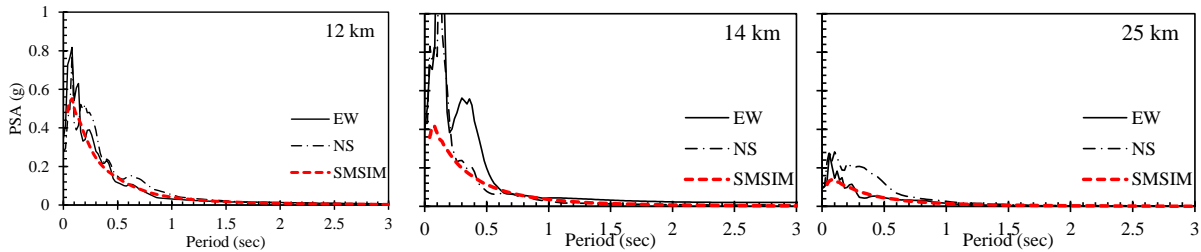


Fig. 16 Response spectra of GMM and Gyeongju Earthquake records

Table 6 $\Delta\sigma$'s of the listed earthquakes (unit: bars)

No.	1	2	3	4	5	6	7	8	9	10	11
$\Delta\sigma$	254	600	500	175	94	26	151	75	76	25	200

Fig. 13 shows the distribution of the residual values showing the best fit to the records of the Gyeongju earthquake when using a stress parameter of 600 bars. Likewise, the value of the stress parameter for the other 10 earthquakes are derived as shown in Table 6. The mean value of the stress parameter for the 11 earthquakes is 198 bars. With the exception of the Gyeongju earthquake of 600 bars, the mean value of the stress parameter is 103 bars.

The average stress parameter of 100 bars for intraplate regions is adopted in several study in Korea (Jo and Baag 2001, 2003, Ha *et al.* 2016) and ENA (Toro *et al.* 1997, Atkinson and Boore 1997).

However, exceptionally high stress drops exceeding 500

Table 7 The values of the GMM parameters used in SMSIM

Density	2.7 gm/cc
S-wave velocity	3.5 km/sec
Partition factor	0.707
Radiation pattern	0.55
Free surface factor	2
Stress parameter	198 bars (600 bars in Sec. 3.2)
Geometrical spreading rate	-1.3 for $R < 70$ km 0.2 for $R < 130$ km -0.5 for $R > 130$ km
Q function	$357f^{-0.5535}$
Duration function (W/O source duration)	0 sec for $R < 10$ km 9.6 sec for $R < 70$ km 7.8 sec for $R < 130$ km (slope) 0.04 for $R > 130$ km
Crustal amplification	1, 1.05, 1.1, 1.2, 1.6, 1.5, 1.3 for 1, 2, 5, 7, 10, 20, 50 Hz
Site diminution κ_0	0.0145 sec

Table 8 Coefficients and standard deviation of GMPE with a stress parameter of 198 bars

T	c_1	c_2	c_3	c_4	c_5	c_6	c_7	c_8	c_9	c_{10}	σ
0.04	-0.840	0.643	-0.0377	-2.78	0.146	-3.71	0.344	- .35	0.121	-0.00104	0.0635
0.05	-0.952	0.653	-0.0361	-2.64	0.128	-3.72	0.339	-1.22	0.104	-0.00109	0.0659
0.075	-1.28	0.683	-0.0347	-2.37	0.102	-3.27	0.299	-0.955	0.0797	-0.00141	0.0710
0.1	-1.63	0.723	-0.0349	-2.18	0.0834	-2.72	0.250	-0.771	0.0642	-0.00166	0.0753
0.15	-2.33	0.864	-0.0435	-1.99	0.0686	-1.88	0.167	-0.631	0.0586	-0.00190	0.0842
0.2	-3.15	1.08	-0.0595	-1.89	0.0605	-1.49	0.122	-0.557	0.0550	-0.00189	0.0915
0.3	-4.76	1.51	-0.0915	-1.73	0.0423	-1.15	0.0858	-0.433	0.0431	-0.00177	0.102
0.4	-6.21	1.92	-0.123	-1.65	0.0351	-1.01	0.0684	-0.368	0.0379	-0.00162	0.110
0.5	-7.48	2.27	-0.149	-1.59	0.0280	-0.964	0.0644	-0.316	0.0318	-0.00151	0.115
0.75	-9.64	2.83	-0.189	-1.50	0.0182	-0.897	0.0582	-0.255	0.0281	-0.00131	0.123
1	-10.8	3.10	-0.205	-1.49	0.0216	-0.885	0.0583	-0.257	0.0322	-0.00118	0.128
1.5	-11.3	3.08	-0.195	-1.58	0.0427	-0.915	0.0677	-0.351	0.0548	-0.001024	0.135
2	-10.9	2.78	-0.165	-1.71	0.0668	-0.966	0.0796	-0.450	0.0738	-0.000924	0.138
3	-9.58	2.17	-0.109	-1.99	0.114	-1.12	0.103	-0.659	0.111	-0.000780	0.142
4	-8.48	1.70	-0.0680	-2.20	0.150	-1.27	0.126	-0.838	0.141	-0.000687	0.142
5	-7.78	1.39	-0.0430	-2.35	0.174	-1.41	0.148	-0.971	0.162	-0.000624	0.141
7.5	-7.00	1.05	-0.0176	-2.61	0.214	-1.67	0.187	-1.24	0.203	-0.000524	0.136
10	-6.92	0.972	-0.0134	-2.71	0.227	-1.87	0.217	-1.35	0.218	-0.000477	0.131

bars in intraplate regions such as ENA are estimated by Boore *et al.* (2010), and are included for determination of the average stress parameter in recent researches of NGA-East (Boore 2015, Pezeshk *et al.* 2015), which is similar to our research.

Fig. 14 shows PSAs of the Gyeongju earthquake records and mean values of PSAs simulated by the GMM with the appropriate values of the parameters at periods of 0.2 sec and 1 sec. Fig. 15 shows comparisons of the acceleration time series of the Gyeongju earthquake with simulated ground motions by using this GMM. The durations of the Gyeongju earthquake records at distance of 12 km are similar to those of the simulated ground motion. Fig. 16 shows the PSAs of the GMM and Gyeongju earthquake records at hypocentral distances of 12 km, 14 km, and 25 km. The PSAs of GMM match well those of the Gyeongju earthquake records at distances of 12 km and 25 km. However, the PSAs of the actual records at distance of 14 km are much larger than those of the GMM. This discrepancy is considered to be due to the ill assumption of the actual soil condition by using soil type B.

3. Development of GMPEs based on stochastically simulated earthquake ground motions

3.1 GMPE by an average stress parameter ($\Delta\sigma=198$ bars)

The synthetic seismograms of 5 earthquakes with moment magnitudes of 4.5, 5, 5.5, 6, and 6.5 were generated for 23 source-to-site distances ranging from 1 km to 800 km (1, 2, 5, 10, 15, 20, 30, 40, 50, 60, 70, 80, 100, 120, 150, 200, 250, 300, 400, 500, 600, 700, and 800 km). 1,000 ground motions are generated for each combination of the magnitude and distance. The values of the GMM parameters given in Table 7 are used for the simulations. The uncertainties in the values of the GMM parameters

could not be accounted for in the derivation of the GMPE, because the number of earthquakes used to develop GMM is not sufficient to have a meaningful estimation of the uncertainty of the values of the GMM parameters. However, the wide range of values in stress parameter as shown in Table 6 is one characteristic of lower-seismicity regions. As Atkinson and Hanks (1995) demonstrate that the standard deviation of a factor related with stress parameter is 0.40 for ENA and 0.18 for California; the corresponding standard deviation of GMPE, is approximately 0.2 for ENA and 0.1 for California. And also this variability affects the sensitivity of GMPE, but is not dealt with herein because it is beyond the scope of this study.

The format of GMPE of Eq. (15) suggested by Atkinson and Boore (2006) is adopted in this study, because it has as many as 10 coefficients to account for all the factors as given in the following.

$$\begin{aligned} \log(PSA) = & c_1 + c_2 M_w + c_3 M_w^2 \\ & + (c_4 + c_5 M_w) (\min(\log R, \log 70)) \\ & + (c_6 + c_7 M_w) (\max(\log(R/130), 0)) \\ & + (c_8 + c_9 M_w) (\max(\log(10/R), 0)) + c_{10} R \\ & + \sigma \end{aligned} \quad (15)$$

where R is the closest distance to the fault. However, the hypocentral distance is used herein. $c_1, c_2, c_3 \dots c_{10}$, and σ are coefficients and standard deviation to be determined in the analysis. c_1 controls spectral acceleration independent of the moment magnitudes and the hypocentral distances. c_2 and c_3 are coefficients only related to the moment magnitudes, and c_{10} related to the hypocentral distances. $c_4 \sim c_9$ are coefficients to control the distance regions, which are divided by trilinear (in log scale) geometrical spreading model of Atkinson (2004) (c_4 and c_5 for $R < 70$ km; c_6 and c_7 for $130 \text{ km} < R$; c_8 and c_9 for $R < 10$ km). This format of equation has evolved from that of Atkinson (2004) to model

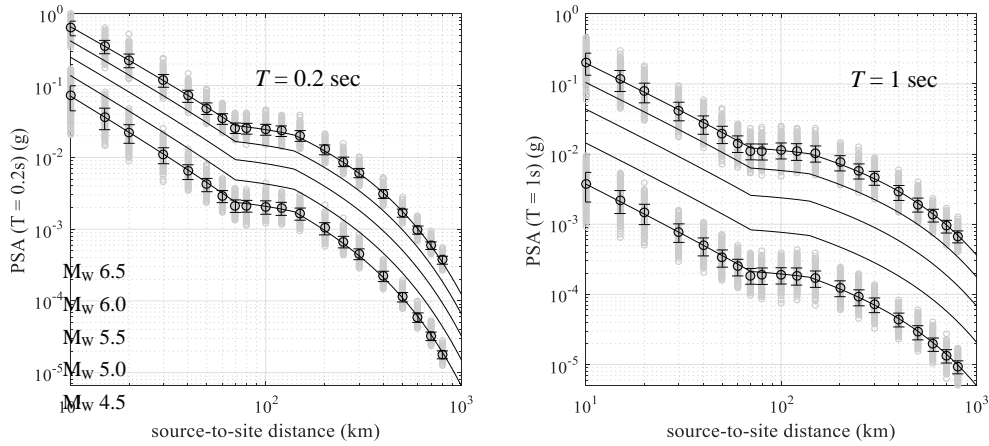


Fig. 17 PSA ($T=0.2$ s and 1 s) distributions of GMPE ($\Delta\sigma=198$ bar) developed by using simulated records. Circle markers show mean values of simulated accelerograms and standard deviation in distance bins. Solid lines are PSAs by GMPE with M_w 4.5, 5, 5.5, 6, and 6.5

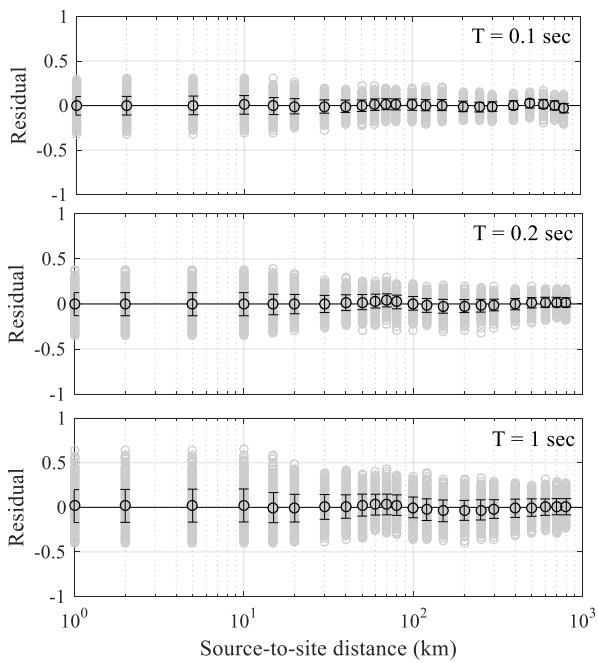


Fig. 18 Residuals versus distance for M_w 6. Gray circles are individual residuals. Hollow circles are mean values of residuals with I marker denoting one standard deviation in each distance bin

the distance region of “offset of decay” from 70 km to 130 km, with the number of c_n increased from 4 to 10.

The result of regression analysis by using *cftool* in MATLAB software are given in Table 8. Fig. 17 shows the PSAs of simulated accelerograms with M_w 4.5 and 6.5, and those by the GMPE with M_w 4.5, 5.0, 5.5, 6.0 and 6.5 at periods of 0.2 sec and 1 sec. The GMPE is shown to be able to represent the simulated accelerograms.

Uncertainties of the GMPE can be divided into epistemic and aleatory uncertainty. The epistemic uncertainty is a degree of inaccuracy caused by insufficient data and misunderstanding, and the aleatory uncertainty is random scatter of the earthquake records.

Atkinson and Boore (2006) did not attempt to model the

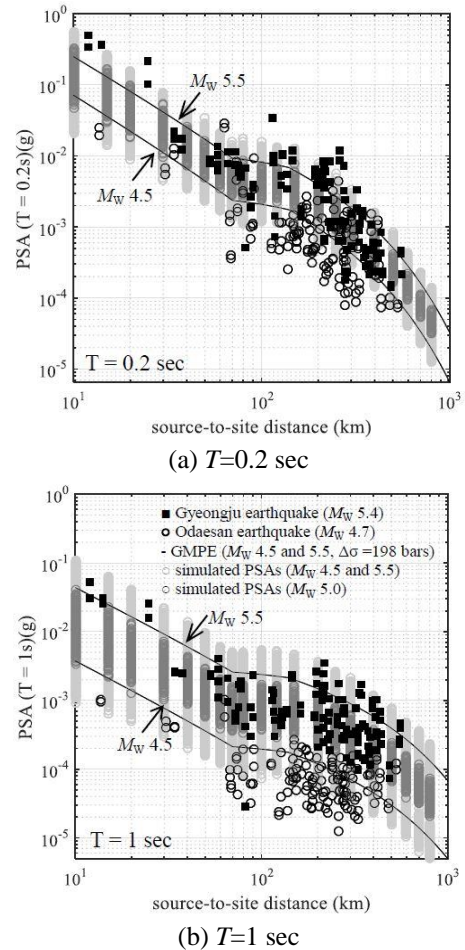


Fig. 19 Comparison of simulated PSAs and GMPE ($\Delta\sigma=198$ bar, lines) corresponding to M_w 4.5 and 5.5 with the Odaesan (M_w 4.7, black circle) and Gyeongju (M_w 5.4, black filled square) earthquakes records. Bright gray is simulated PSA with M_w 4.5 and 5.5, and dark gray is those with M_w 5.0

effects of the epistemic uncertainty in a comprehensive way in their simulations, because they do not believe this would be an appropriate way to deal with the broader issue of epistemic

uncertainty in GMPEs. To properly consider epistemic uncertainty, one needs to consider a wide variety of alternative models and theories of ground motion, which is beyond their scope that is limited to defining their estimate of the ground motions for ENA and aleatory uncertainty of their GMPE due to the natural random variability in earthquake source, path and site effects. Likewise, epistemic uncertainty is not considered in this study.

Aleatory uncertainty is quantified as the standard deviation of simulated records. The standard deviations of the developed GMPE do not exceed 0.2 log units at all periods. Atkinson and Boore (2006) noted that uncertainty value of 0.3 log units determined from their study is slightly larger than the typically observed values for empirical ground motion equations in California. The relatively lower aleatory uncertainty of the GMPE developed in this study is considered due to the use of the fixed values of GMM parameters without accounting for their own uncertainty. Fig. 18 shows the residual distributions at periods of 0.1 sec, 0.2 sec, and 1 sec.

Fig. 19 shows a comparison of the GMPE with records of the Gyeongju (M_w 5.4) and Odaesan (M_w 4.7) earthquakes. PSAs of the GMPE at the near-source distances are lower than those of the Gyeongju earthquake at the period of 0.2 sec, but, generally match well the actual records over the whole distance range. At the period of 1 sec, the GMPE predicts generally larger PSAs than those of the earthquake records.

3.2 The GMPE with $\Delta\sigma=600$ bars obtained for the Sept. 12, 2016 Gyeongju earthquake

The mean value of the stress parameter, 198 bar, derived from the records of the 11 earthquakes is not considered to be statistically meaningful, because the number of earthquakes in that bin is small especially for higher magnitudes.

However, it is meaningful to see how much difference the

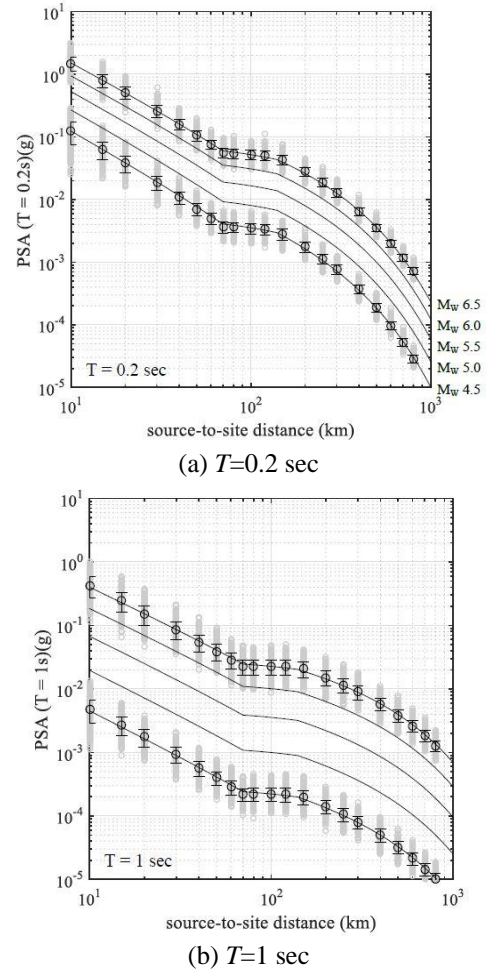


Fig. 20 PSA ($T=0.2$ s and 1 s) distributions of GMPE developed by using simulated records with $\Delta\sigma=600$ bar. Circle markers and horizon bar denote mean values of simulated accelerograms and standard deviation in distance bins. Solid lines are PSAs by GMPE with M_w 4.5, 5, 5.5, 6, and 6.5

Table 9 Coefficients and standard deviation of GMPE with a stress parameter of 600 bars

T	C ₁	C ₂	C ₃	C ₄	C ₅	C ₆	C ₇	C ₈	C ₉	C ₁₀	σ
0.04	-0.697	0.702	-0.040	-2.76	0.137	-4.00	0.394	-1.28	0.104	-0.00117	0.0644
0.05	-0.859	0.719	-0.039	-2.59	0.115	-3.95	0.385	-1.14	0.0861	-0.00125	0.0672
0.075	-1.27	0.759	-0.037	-2.28	0.083	-3.32	0.324	-0.842	0.0582	-0.00162	0.0743
0.1	-1.82	0.867	-0.043	-2.10	0.068	-2.66	0.256	-0.706	0.0518	-0.00186	0.0793
0.15	-2.89	1.14	-0.064	-1.94	0.059	-1.78	0.158	-0.593	0.0503	-0.00202	0.0882
0.2	-4.03	1.45	-0.086	-1.82	0.046	-1.41	0.115	-0.496	0.0423	-0.00198	0.0958
0.3	-6.16	2.04	-0.131	-1.67	0.031	-1.11	0.0787	-0.380	0.0319	-0.00180	0.106
0.4	-7.79	2.49	-0.165	-1.61	0.025	-1.01	0.0669	-0.331	0.0295	-0.00163	0.114
0.5	-8.98	2.80	-0.187	-1.58	0.023	-0.938	0.0592	-0.324	0.0314	-0.00152	0.118
0.75	-10.6	3.14	-0.207	-1.56	0.028	-0.929	0.0615	-0.319	0.0377	-0.00132	0.125
1	-11.0	3.15	-0.201	-1.59	0.036	-0.928	0.0652	-0.337	0.0448	-0.00120	0.129
1.5	-10.5	2.76	-0.161	-1.79	0.076	-0.987	0.0781	-0.504	0.0787	-0.00104	0.134
2	-9.45	2.30	-0.120	-2.00	0.113	-1.09	0.0965	-0.676	0.109	-0.00092	0.135
3	-7.99	1.68	-0.066	-2.32	0.167	-1.28	0.125	-0.929	0.152	-0.00077	0.137
4	-7.14	1.32	-0.038	-2.55	0.203	-1.44	0.148	-1.13	0.185	-0.00067	0.135
5	-6.73	1.14	-0.025	-2.68	0.224	-1.57	0.167	-1.26	0.206	-0.00062	0.134
7.5	-6.55	1.00	-0.017	-2.85	0.246	-1.85	0.209	-1.44	0.229	-0.000534	0.129
10	-6.75	1.01	-0.019	-2.89	0.247	-2.02	0.233	-1.49	0.232	-0.000490	0.125

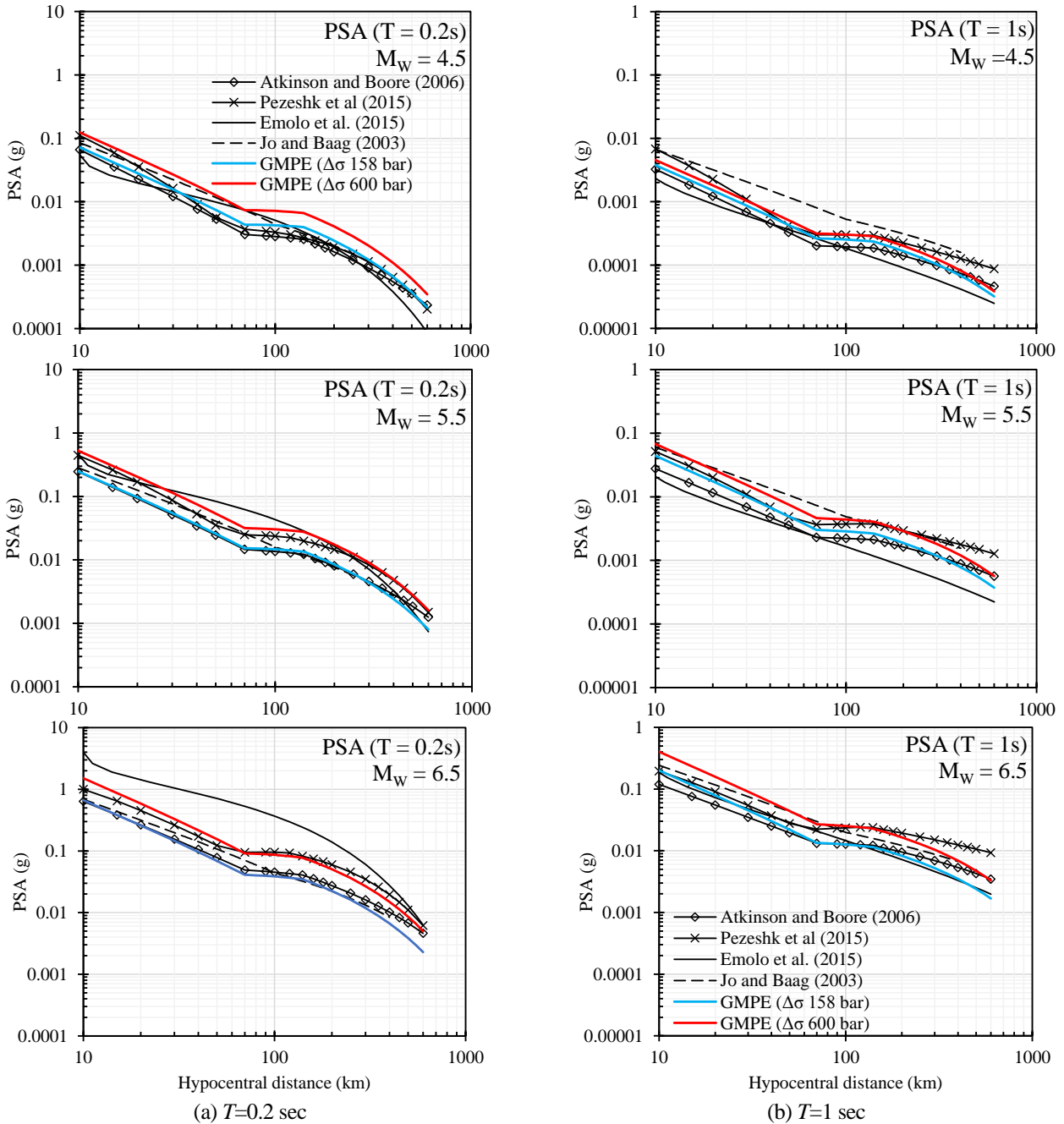


Fig. 21 Comparison of PSAs by GMPEs of this study (solid blue lines=GMPE with $\Delta\sigma=198$ bar, solid red lines indicate the GMPE with $\Delta\sigma=600$ bar) for M_w 4.5, 5.5, and 6.5, with predictions for ENA (Atkinson and Boore 2006, Pezeshk *et al.* 2015) and Korea (Emolo *et al.* 2015)

GMPE with the stress parameter of the Gyeongju earthquake, 600 bars, makes compared to the GMPE with that of 198 bars for reference. The GMPE with a stress parameter of 600 bars and others being the same as that shown in Table 9, and PSAs of simulated ground motion with mean values and standard deviations are given in Fig. 20.

Fig. 21 shows a comparison of the GMPEs with stress parameters of 198 bar and 600 bar (hereafter S198 and S600, respectively), and GMPEs for lower seismicity regions by Atkinson and Boore (2006), Pezeshk *et al.* (2015) (hereafter AB06, and P15) for ENA. However, the GMPE-P15 is calibrated to empirical earthquake record by a hybrid empirical

method (HEM) in their study. Adjustment factors based on simple seismological models to account for differences in anelastic attenuation and regional magnitude measures between the host and target regions are used to develop the GMPE in the hybrid empirical method. The GMPE by Jo and Baag (2003) (hereafter JB03) is derived by simulated ground motions based on 44 records of 16 earthquakes in south-eastern Korea. However, the GMPE by Emolo *et al.* (2015) (hereafter E15) is based on empirical earthquake records with the local magnitude ranging from 2.0 to 5.1 in Korea. Stress parameters of 140 bars, 400 bars and 92 bars are used in the GMPE-AB06, P15, and JB03, respectively.

Table 10 PSAs of the GMPEs shown in Fig. 21 (unit: g)

GMPE	$T=0.2$ sec		$T=1$ sec		
	R_{HYPO} (km)		R_{HYPO} (km)		
	20	70	20	70	
$M_W 5.5$					
Korea	S198	0.097	0.0153	0.0174	0.00301
	S600	0.204	0.0317	0.0268	0.00461
	JB03	0.126	0.0262	0.0287	0.00731
	E15	0.116	0.0623	0.0081	0.00233
ENA	AB06	0.093	0.0146	0.0115	0.00229
	P15	0.169	0.0202	0.0201	0.00366
$M_W 6.5$					
Korea	S198	0.259	0.0410	0.0787	0.0134
	S600	0.586	0.0915	0.158	0.0269
	JB03	0.315	0.0705	0.116	0.0298
	E15	1.416	0.530	0.0724	0.0208
ENA	AB06	0.264	0.0490	0.0551	0.0132
	P15	0.452	0.0903	0.0903	0.0223

The PSAs of 6 GMPEs for $M_W 4.5$ are not much different. The ground motions with $M_W 4.5$ are not of engineering interest because the PSA values caused by this magnitude are too low to cause damage to building structures. Thus, detailed comparison of the above GMPEs with $M_W 4.5$ are not discussed.

Table 10 shows the PSAs of the GMPEs with $M_W 5.5$ and 6.5 at the hypocentral distances (R_{HYPO}) of 20 km and 70 km. One of the objectives in this study is to predict the ground motions with $M_W \geq 6.5$ by using earthquake records with $M_W \leq 5.5$ in Korea.

PSAs of GMPE-S600, which represents the ground motions with the highest stress parameter in Korea fitting best the three exceptionally high PSAs at the nearest epicentral distances, are much larger than those of the GMPE-AB06 and -P15 for ENA. In addition, PSAs of the GMPE-S600 are twice as large as those of the GMPE-S198, and, are considered to be inappropriate for the seismic design spectrum.

The short-period PSAs of GMPE-E15 are 5 times larger than those of the GMPE-S198 with $M_W 6.5$ at a distance of 70 km. GMPE-E15 cannot be used either due to these conservative PSAs at a period of 0.2 sec for $M_W 6.5$, because these PSA values are obtained by mere extrapolation from the range of the local magnitude, 2.0~5.1. PSAs of GMPE-JB03 are generally 1.5 times larger than those of GMPE-S198 at the distances of 20 km and 70 km. GMPE-S198 shows lower PSA values than the other GMPEs at short period of 0.2 sec, and the long-period PSAs of GMPE-S198 at a distance of less than 100 km are between those of the GMPEs for ENA.

In summary, the GMPE-S198 does a reasonable job of predicting the PSAs in Korea in spite of its general lower PSAs than GMPE-E15 and -JB03.

3.3 Comparison of the GMPE-S198 with the design spectrum of KBC

Strong ground motions for the Korean peninsula can be predicted by using the GMM or GMPE. Fig. 24 shows examples of the simulated strong ground motions time series

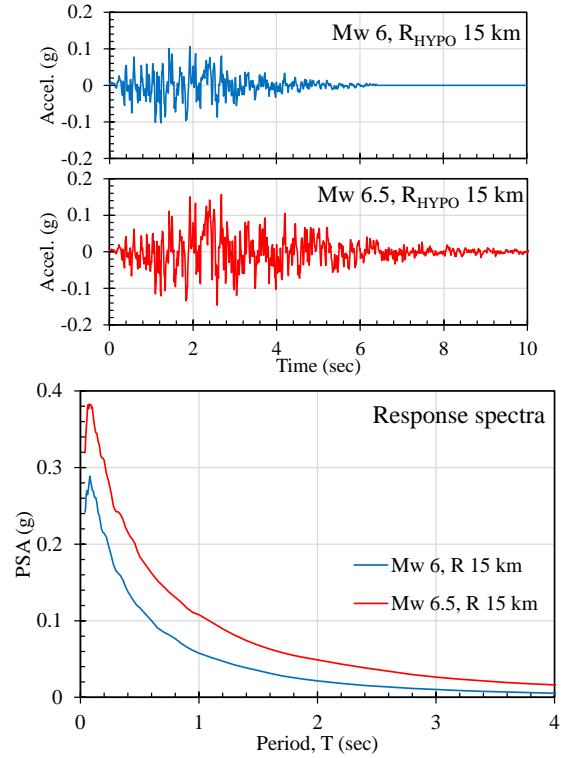


Fig. 24 Simulated ground motions with $M_W 6 - R_{HYPO}$ 15 km and with $M_W 6.5 - R_{HYPO}$ 20 km ($\Delta\sigma=198$ bar)

and the median response spectra of 200 simulations with $M_W 6 - R_{HYPO}$ 15 km and with $M_W 6.5 - R_{HYPO}$ 15 km, which are of engineering interest in the magnitude and distance range in seismic hazard analysis or structural design. The PGAs of those strong ground motions are 0.1 g or larger. The durations of ground motion of $M_W 6 - R_{HYPO}$ 15 km and $M_W 6.5 - R_{HYPO}$ 20 km are about 6 sec and 10 sec, respectively.

Fig. 25 compares PSAs obtained from mean +1 sigma values of the developed GMPE ($\Delta\sigma=198$ bar) with the design spectrum of the KBC. The soil condition assumed in the GMPE and that of the design spectrum are S_B ($V_{S,30}=760$ m/s ~ 1,500 m/s). The PSAs of the GMPE with $M_W 6.5 - R_{HYPO}$ 15 km are 1.5 times larger than the design spectrum of KBC at the period of 0.1 sec, but similar to values of PSAs at periods beyond 0.4 sec. SDs of the GMPE at the periods longer than 2 sec do not exceed 8 cm. The PSAs and SDs of the GMPE with $M_W 6.5 - R_{HYPO}$ 15 km generally match to design spectrum of KBC 2016.

The PSA of the GMPE at a short period of 0.1 s decreased by half with the increase of the hypocentral distance from 15 to 25 km, thereby showing a rapid decay of the high frequency. The PSAs of the GMPE with an M_W of 6.5 - R_{HYPO} of 25 are much lower than those of the KBC.

While the short-period PSAs with an $M_W 6.0$ are approximately 70% of those of an $M_W 6.5$, long-period SD's of an $M_W 6.0$ is approximately only 40% of those of the $M_W 6.5$. This finding means that long-period SD is more sensitive to the magnitude.

Therefore, building structures designed according to KBC seem to be capable of sustaining the ground motions with an $M_W 6.5$ and with a hypocentral distance that is beyond approximately 15 km. In other words, the PSAs indicate that at

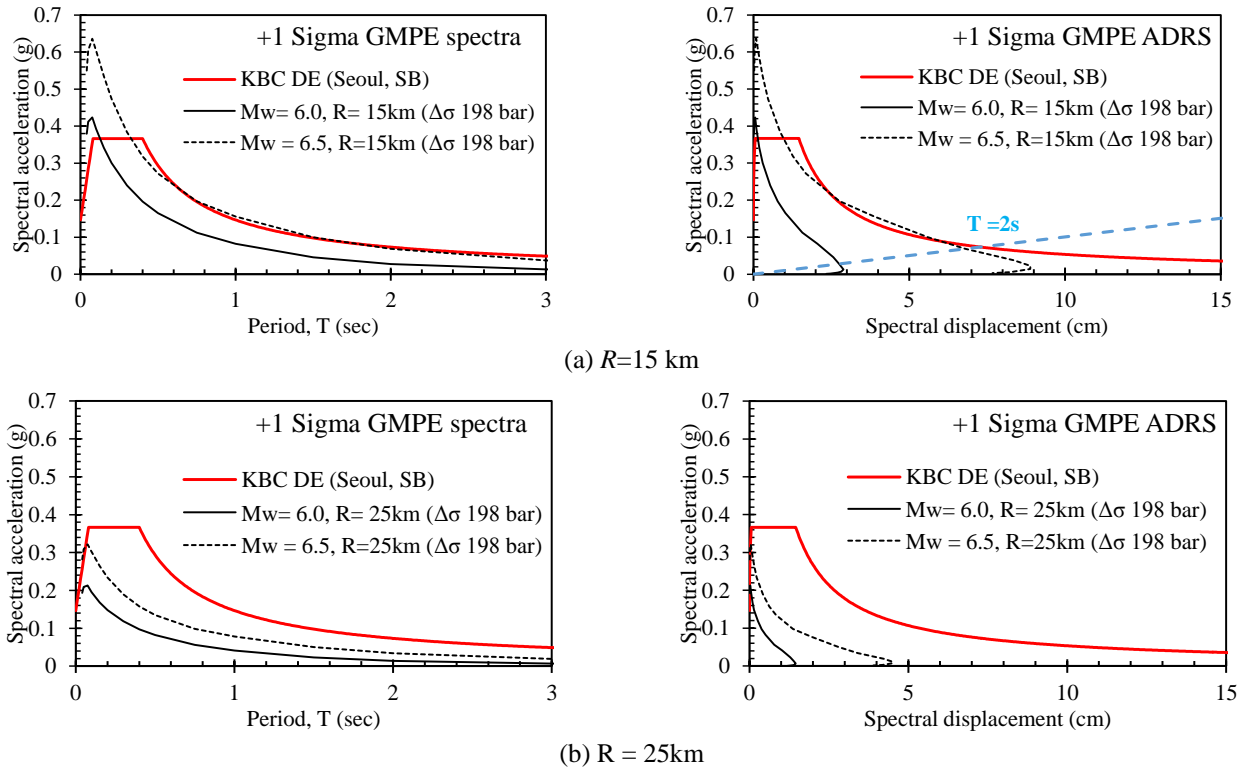


Fig. 25 Comparison of response spectra of the GMPE ($\Delta\sigma=198$ bars) with M_w 6 and 6.5 at the hypocentral distances of (a) 15 km and (b) 25 km, and the design spectrum of KBC (2016)

25 km distance, earthquakes with magnitude of 6.5 or less do not represent damage to structures, if the structure were designed and constructed according to the current seismic code in KBC2016.

The design spectrum of the building codes is based on qualitative evaluations of PSHA (Lam *et al.* 2016, Atkinson 2004b). Although this comparison of the design spectrum with those of the GMPE developed herein intends to identify the characteristic of the scenario earthquake in a lower-seismicity region such as South Korea, it does not mean that the current design spectrum should be modified accordingly. To develop a design spectrum compatible with the Korean Peninsula, more systematic research using probabilistic seismic hazard analysis is necessary in the future.

4. Conclusions

GMPEs, giving ground-motion intensity measures such as peak ground motions or response spectra as a function of earthquake magnitude and distance, are important tools in the analysis of seismic hazard (Boore and Atkinson 2008) and seismic design.

For the high seismicity regions such as western North America, the GMPEs are developed by empirical regression analysis of the database of recorded ground-motion (Boore and Atkinson 2008, Power *et al.* 2006). For low-to-moderate seismicity regions such as eastern North America, earthquake records are insufficient in magnitude and distance range to be of engineering interest to develop GMPEs using empirical regression analysis (Atkinson

2008). Because of this lack of records from moderate earthquake, the GMPEs for lower seismicity regions have been developed by using synthetic ground motions instead of empirical earthquake records. In this study, synthetic ground motions are generated using the GMM developed for the Korean Peninsula, for which the parameters were calibrated with records of the 11 recent earthquakes of $M_L > 4.5$ in Korea including the Gyeongju earthquake on Sept. 12, 2016 (M_L 5.8), the largest earthquake since seismic instrumental recording began in 1978 in Korea.

The parameters of the GMM for each of the earthquakes are derived as follows: (1) Upper-crust amplification factor for generic rock ($V_{s,30}=750$ m/s \sim 1,500 m/s, S_B) proposed by Kim and Yoon (2006) are used. (2) κ_0 is given by the slope of the Fourier spectral decay for frequency ranges from 10 Hz to 25 Hz. (3) Geometrical spreading of $R^{-1.5}$ within the distance of 70 km is selected based on the regression of $PSA_{0.2s}$. (4) $Q_0 f^{-\eta}$ of anelastic attenuation factor is derived by the inversion using the GMM with tentative value of $\Delta\sigma$ 200 bars. (5) $\Delta\sigma$ is re-estimated by reducing the residuals, $\log(PSA_{0.2s}^{OBS}/PSA_{0.2s}^{SIM})$ to the minimum. The uncertainties in the values of the GMM parameters could not be accounted for in the derivation of the GMPE, because the number of earthquakes used to develop the GMM is insufficient to have a meaningful estimation of the uncertainty on the values of GMM parameters.

The GMPE is developed by using synthetic ground motions based on the GMM with mean values of the above parameters. 1000 simulations are conducted to generate ground motions for each moment magnitude ranging from 4.5 to 6.5, and hypocentral distance ranging from 1 km to

800 km by using SMSIM (Boore 2005). An equation for GMPE containing 10 constants proposed by Atkinson and Boore (2006) is used.

The GMPE-S198 bars does a reasonable job of predicting the PSAs for lower seismicity regions, although that has generally lower PSAs than E15 and JB03 model. The short-period PSAs of the GMPE-S198 bars are equal to or lower than those of GMPE-AB06, and much lower than those of GMPE-P15. The long-period PSAs of the GMPE-S198 at a distance of less than 100 km are between those of the GMPE-AB06 and -P15.

PSAs of $+1\sigma$ GMPE with M_W 6.5 at hypocentral distance of 15 km and 25 km are compared to the design spectrum of the Korean Building Code 2016 (KBC) with soil condition, S_B . The design spectrum of the KBC 2016 generally corresponds to PSAs and SDs of GMPE with M_W 6.5- R_{HYPO} 15 km and the response characteristics of M_W 6.5 earthquakes at the distance of 15 km expected in the Korean Peninsula are: (1) PSAs at short periods can be 1.5 times larger than KBC accelerations. (2) SDs at the long periods larger than 2 sec do not exceed 8 cm for soil condition, S_B .

PSAs of the GMPE at a short period decrease to half with the hypocentral distance increasing from 15 km to 25 km showing a rapid decay in high frequency. PSAs of the GMPE with M_W 6.5 at a distance of 25 km are much lower than those by KBC. Therefore, building structures designed according to KBC2016 seem to be capable of sustaining ground motions with M_W 6.5 beyond a hypocentral distance of about 15 km.

Acknowledgments

This research was supported by a grant (17AUDP-B066083-05) from the Architecture & Urban Development Research Program funded by the Ministry of Land, Infrastructure and Transport of the Korean government.

References

- AIK Korean Building (2016), "KBC 2016", Architectural Institute of Korea, Seoul, Korea.
- Al Atik, L., Abrahamson, N., Bommer, J.J., Scherbaum, F., Cotton, F. and Kuehn, N. (2010), "The variability of ground-motion prediction models and its components", *Seismol. Res. Lett.*, **81**(5), 794-801.
- Anderson, J.G. and Hough, S.E. (1984), "A model for the shape of the Fourier amplitude spectrum of acceleration at high frequencies", *Bull. Seismol. Soc. Am.*, **74**(5), 1969-1993.
- Atkinson, G.M. (2004a), "Empirical attenuation of ground-motion spectral amplitudes in southeastern Canada and the northeastern United States", *Bull. Seismol. Soc. Am.*, **94**(3), 1079-1095.
- Atkinson, G.M. (2004b), "An overview of developments in seismic hazard analysis", *Proceedings of the 13th World Conference on Earthquake Engineering*, Paper No. 5001.
- Atkinson, G.M. (2008), "Ground-motion prediction equations for eastern North America from a referenced empirical approach: implications for epistemic uncertainty", *Bull. Seismol. Soc. Am.*, **98**(3), 1304-1318.
- Atkinson, G.M. and Boore, D.M. (1995), "Ground-motion relations for eastern North America", *Bull. Seismol. Soc. Am.*, **85**(1), 17-30.
- Atkinson, G.M. and Boore, D.M. (1997), "Some comparisons between recent ground motion relations", *Sesimol. Res. Lett.*, **68**(1), 24-40.
- Atkinson, G.M. and Boore, D.M. (2006), "Earthquake ground-motion prediction equation for eastern North America", *Bull. Seismol. Soc. Am.*, **96**(6), 2181-2205.
- Atkinson, G.M. and Hanks, T.C. (1995), "A high-frequency magnitude scale", *Bull. Seismol. Soc. Am.*, **85**(3), 825-833.
- Boore, D.M. (2003), "Simulation of ground motion using the stochastic method", *Pure Appl. Geophys.*, **160**, 635-676.
- Boore, D.M. (2005), "SMSIM-Fortran programs for simulating ground motions from earthquakes: version 2.3-A revision of OFR 96-80-A", US Geological Survey open-file Report 00-509, August.
- Boore, D.M. (2015), "Point-source stochastic-method simulations of ground motions for the PEER NGA-East project", Pacific Earthquake Engineering Research Center (PEER), Report PEER 2015/04, April.
- Boore, D.M. and Atkinson, G.M. (2008), "Ground-motion prediction equations for the average horizontal component of PGA, PGV, and 5%-damped PSA at spectral periods between 0.01s and 10.0s", *Earthq. Spectra*, **24**(1) 99-138.
- Boore, D.M. and Joyner, W.B. (1997), "Site amplifications for generic rock sites", *Bull. Seismol. Soc. Am.*, **87**(2), 327-341.
- Boore, D.M., Campbell, K.W. and Atkinson, G.M. (2010), "Determination of stress parameters for eight well-recorded earthquakes in Eastern North America determination of stress parameters for eight well-recorded earthquakes in Eastern North America", *Bull. Seismol. Soc. Am.*, **100**(4), 1632-1645.
- Boore, D.M., Campbell, K.W. and Atkinson, G.M. (2010), "Determination of stress parameters for eight well-recorded earthquakes in eastern North America", *Bull. Seismol. Soc. Am.*, **100**(4), 1632-1645.
- Boore, D.M., Stewart, J.P., Seyhan, E. and Atkinson, G.M. (2014), "NGA-West2 equations for predicting PGA, PGV, and 5% damped PSA for shallow crustal earthquakes", *Earthq. Spectra*, **30**(3), 1057-1085.
- Brune, J.N. (1970), "Tectonic stress and the spectra of seismic shear waves from earthquakes", *J. Geophys. Res.*, **75**(26), 4997-5009.
- Choi, H., Noh, M. and Choi, K. (2004), "The relation between local magnitude and moment magnitude in the southern part of the Korean Peninsula", *J. Korean Geophys. Soc.*, **7**(3), 185-192.
- Darragh, R.B., Abrahamson, N.A., Silva, W.J. and Gregor, N. (2015), "Development of hard rock ground motion models for region 2 of central and eastern North America", NGA-East: Median Ground-Motion Models for the Central and Eastern North America Region, PEER Report No. 201504, 51-84.
- Electric Power Research Institute (EPRI), Guidelines for Site Specific Ground Motions, Palo Alto, California, Electric Power Research Institute, TR-102293, November.
- Emolo, A., Sharma, N., Festa, G., Zollo, A., Concertito V., Park, J., Chi, H. and Lim, I (2015), "Ground-motion prediction equation for south Korea Peninsula", *Bull. Seismol. Soc. Am.*, **105**(5), 2625-2640.
- Frankel, A. (1995), "Mapping seismic hazard in the central and eastern United States", *Seismol. Res. Lett.*, **66**(4), 8-21.
- Ha, S.J., Jee, H.W. and Han, S.W. (2016), "Simulation of ground motions from Gyeongju earthquake using point source model", *J. Earthq. Eng. Soc. Korea*, **20**(7) 537-543.
- Hanks, T.C. (1982), " f_{max} ", *Bull. Seismol. Soc. Am.*, **72**(6A), 1867-1879.
- Hanks, T.C. and Kanamori, H. (1979), "A moment magnitude scale", *J. Geophys. Res.*, **84**(B5), 2348-2350.
- Jo, N.D. and Baag, C.E. (2001), "stochastic prediction of strong ground motions in southeastern Korea", *J. Earthq. Eng. Soc. Korea*, **5**(4), 17-26.
- Jo, N.D. and Baag, C.E. (2003), "Estimation of spectrum decay

- parameter κ and stochastic prediction of strong ground motions in southeastern Korea”, *J. Earthq. Eng. Soc. Korea*, **7**(6), 59-70.
- Joyner, W.B., Warrick, R.E. and Fumal, T.E. (1981), “The effect of Quaternary alluvium on strong ground motion in the Coyote Lake, California, earthquake of 1979”, *Bull. Seismol. Soc. Am.*, **71**(4), 1333-1349.
- Kim, D.S. and Yoon, J.K. (2006), “Development of new site classification system for the regions of shallow bedrock in Korea”, *J. Earthq. Eng.*, **10**(03), 331-358.
- Lam, N., Tsang, H., Lumantarna, E. and Wilson, J. (2016), “Minimum loading requirements for areas of low seismicity”, *Earthq. Struct.*, **11**(4), 539-561.
- Lam, N., Wilson, J. and Hutchinson, G. (2000), “Generation of synthetic earthquake accelerograms using seismological modelling: a review”, *J. Earthq. Eng.*, **4**(3), 321-354.
- NIMR (2014), Analysis of Site Environment at Permanent Seismic Stations Operated by Korea Meteorological Administration, National Institute of Meteorological Research, Report No. NIMR-TN-2014-007, August.
- Pezeshk, S., Zandieh, A. and Tavakoli, B. (2011), “Hybrid empirical ground-motion prediction equations for eastern North America using NGA models and updated seismological parameters”, *Bull. Seismol. Soc. Am.*, **101**(4), 1859-1870.
- Pezeshk, S., Zandieh, A., Campbell, K.W. and Tavakoli, B. (2015), “Ground-motion prediction equations for CENA using the hybrid empirical method in conjunction with NGA-West2 empirical ground-motion models”, Pacific Earthquake Engineering Research Center (PEER) report PEER 2015/04. April.
- Toro, G., Norman, A. and John, S. (1997), “Model of strong ground motions from earthquakes in Central Eastern North America: Best estimate and uncertainties”, *Seismol. Res. Lett.*, **68**(1) 41-57.
- Yenier, E. and Atkinson, G.M. (2015), “An equivalent point-source model for stochastic simulation of earthquake ground motions in California”, *Bull. Seismol. Soc. Am.*, **105**(3), 1432-1455
- Zuccolo, E., Bozzoni, F. and Lai, C.G. (2017), “Regional low-magnitude GMPE to estimate spectral accelerations for earthquake early warning applications in Southern Italy”, *Seismol. Res. Lett.*, **88**(1), 61-71.